P5.16

AN AUTOMATED ALGORITHM FOR RADAR BEAM OCCULTATION

Carrie Langston[1], Jian Zhang[1]
[1]Cooperative Institute for Mesoscale Meteorological Studies, Norman, OK

1. INTRODUCTION

The deployment of the Weather Surveillance Radar – 1988 Doppler (WSR-88D) network has provided weather forecasters critical information for issuing warnings on the occurrence of tornadoes, severe storms, and flash floods. Accurate beam blockage information is very important to all radar data applications, especially in mountainous regions (Westrick et al., 1999; Pellarin et al., 2002). Kucera et al. (2004) developed a technique that uses high-resolution DEM (digital elevation model) data and a radar beam propagation model to calculate beam occultations. The technique was used to study the GUAM radar beam blockage patterns.

The National Severe Storms Laboratory (NSSL) has developed an automated algorithm, HybScan, that calculates beam occultation and hybrid elevation angles based on terrain, radar beam pattern (or power density function), and radar beam propagation path. The NSSL HybScan algorithm uses similar techniques as in Kucera et al. (2004) but to develop a "hybrid scan" (O'Bannon, 1997) of lowest radar beams that are not significantly blocked by terrain. The hybrid scan is used in the operational WSR-88D precipitation process system (PPS) (Fulton et al. 1998) to derive rainfall products. The HybScan algorithm has been used to develop beam occultation and hybrid elevation angle data sets for all the WSR-88D radars using 1 arc seconds DEM data. The algorithm is independent of radar types (e.g., WSR-88D, Terminal Doppler Weather Radar, etc) and of radar scan strategies.

Parameters for the algorithm mentioned previously will be presented in section 2, the algorithm in section 3, and sample results in section 4 with a summary in section 5.

2. PARAMETERS

The HybScan algorithm uses several adaptable parameters and high-resolution terrain data (DEM) to create customized beam occultation and hybrid elevation angle data sets. Adaptable parameters include grid size and resolution. For a WSR-88D, a grid size of 360°× 300 km with a resolution of 1°× 1 km is the default setting.

The algorithm can generate hybrid elevation angles using different criteria sets. User defined thresholds for beam bottom clearance and occultation define the criteria for a hybrid elevation angle, which is the lowest angle satisfying both requirements. Beam bottom clearance is the height that a radar beam's bottom passes above the terrain (Fig. 1). Occultation is the percent of the radar beam power lost due to beam blockage. The power lost is based on a radar power density function, which is a Bessel function of 2nd order (Doviak and Zrnic, 1993) (Fig. 2). Terrain blocking center portions of the beam will reduce the beam power more so than terrain blocking outer portions of the beam. For WSR-88D's, a beam bottom clearance of 50 m or more and an occultation of less than 60% are used to define a hybrid elevation angle. The quality of the terrain data and the settings for both beam bottom clearance and occultation can greatly influence the outcome of the HybScan algorithm.

3. ALGORITHM

The HybScan algorithm uses DEM data and a set of adaptable parameters to calculate a hybrid elevation angle data set for a given radar's coverage map. The algorithm begins by remapping Cartesian DEM data to a high-resolution polar grid centered on a specified radar location. This high-resolution grid is user defined and used to perform beam blockage and occultation calculations. For WSR-88D's, a high grid resolution of 0.1°× 100 m is the default setting. HybScan is capable of using multiple DEM's to build one high-resolution polar grid. Upon remapping the high-resolution terrain data, the algorithm calculates the hybrid elevation angle for each bin.

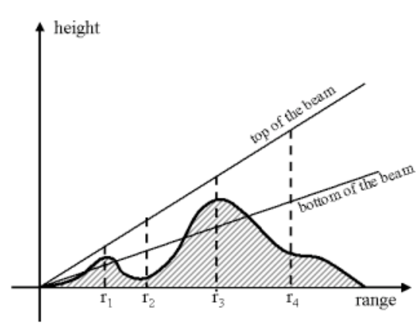

Fig. 1 Radar beam blockage illustrating how terrain, beam top, and beam bottom can relate. At reference points r_2 and r_4 the beam bottom clears the ground. However, the beam bottom falls below the terrain at r_1 and r_3, blocking portions of the beam.

Corresponding author address: Carrie Langston, NSSL, 1313 Halley Circle, Norman, OK 73069.
Email: carrie.langston@noaa.gov

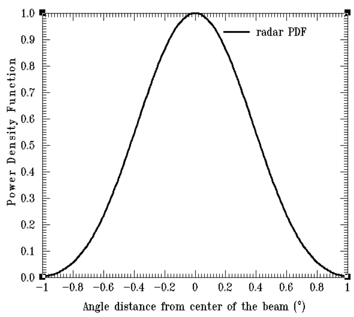

Fig. 2 Radar power density function used to calculate radar beam power loss.

To compute the hybrid elevation angle, the algorithm calculates the elevation angle of a beam that clears the terrain by the beam bottom clearance threshold (i.e., terrain MSL + 50 m), assuming radar beams propagate under standard atmospheric refraction conditions, i.e.:

$$\theta = \sin^{-1}\left[\frac{h^2 - r^2 + 2a_e \bullet h}{2a_e r}\right] \tag{1}$$

where h is the elevation, r is the slant range from the radar, a_e is 4/3 earth's radius, and θ is the elevation angle.

Note that equation (1) was derived from the equation (2.28b) in Doviak and Zrnic (1993).

The beam blockage and occultation are calculated using the elevation angle as a first guess. If the occultation is less than the threshold (60%) then the hybrid elevation has been found. Otherwise, the algorithm increases the elevation angle and performs the beam blockage and occultation calculations again. The algorithm will continue to adjust the elevation angle in an iterative process until finding the hybrid elevation angle. Note the beam blockage calculation is global. The current bin's beam blockage cannot be less than that of the previous bin.

The algorithm writes out a polar grid of hybrid elevation angles and may also output several optional fields such as the polar DEM grid

4. EXAMPLES

Two examples of HybScan output are given in this section. These examples each include the polar DEM data used to calculate the hybrid elevation angles and the hybrid elevation angles themselves. In addition, the hybrid scan for VCP 12 is given. These are compared to the operation hybrid scan currently used in the WSR-88D PPS.

The WSR-88D based in Denver, Colorado, KFTG, serves as the first example. Fig. 3 shows the polar DEM grid for KFTG. From this grid, the hybrid elevations angles are computed using a beam bottom clearance of 50 m and an occultation threshold of 60%. They are plotted in Fig. 4. Using the hybrid elevation angle data, the hybrid scan can be determined for any scan strategy. In this instance, the hybrid scan for VCP 12 (Fig. 5a) is computed. Comparing the hybrid scan in Fig. 5a to the operational hybrid scan (Fig. 5b), several differences are noticeable.

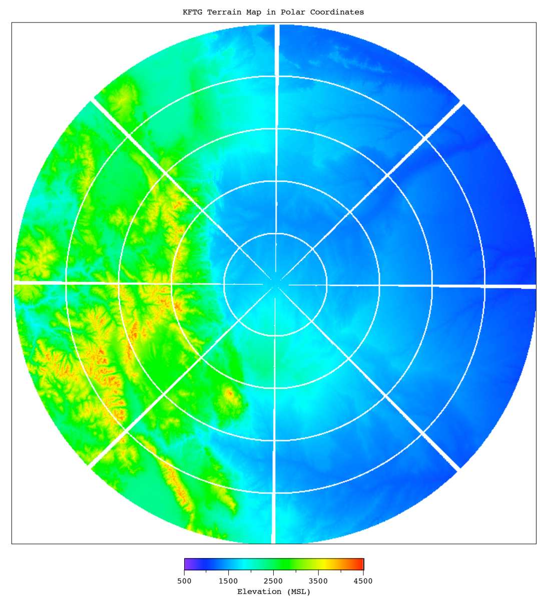

Fig. 3 A polar DEM grid as remapped from a Cartesian grid for KFTG. Range rings are every 50 km and azimuths every 45°.

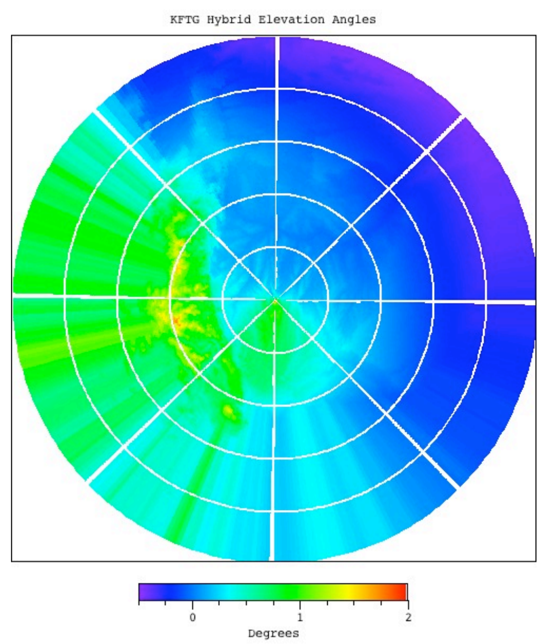

Fig. 4 The hybrid elevation angles for KFTG. Range rings are every 50 km and azimuths every 45°.

The hybrid scan of VCP 12 for KFTG is markedly different than the operation hybrid scan. East of KFTG, there is an increase in tilt number, and terrain features are more sharply outline by changes in tilt number. This is due to the higher resolution terrain data used by HybScan to generate the hybrid elevation angles. Lower tilt numbers are seen in the operational hybrid scan due to an elevation angle resolution that is courser than VCP 12 at lower levels.

Operational hybrid scans are used for VCP 11, 21, 31, and 32. The four corresponding lowest elevation angles used in these VCP's are approximately equal. Thus, operational hybrid scans are limited to the four lowest tilts. Table 1 lists several VCP's and their corresponding elevation angles.

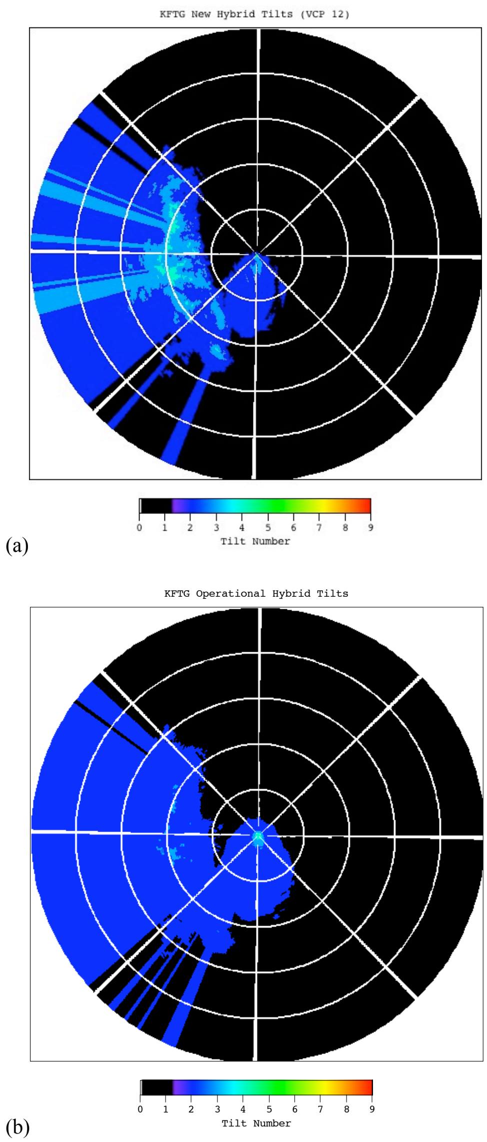

Fig. 5 Hybrid scan for KFTG generated for VCP 12 (a) and for operational WSR-88D hybrid scan (b). Range rings are every 50 km and azimuths every 45°.

The WSR-88D based in Phoenix, Arizona, KIWA, is the second example. The polar DEM grid (Fig. 6), hybrid elevation angles (Fig. 7), hybrid scan for VCP 12 (Fig. 8a), and the operational hybrid scan (Fig. 8b) are given. Noticeable differences between Fig. 8a and Fig. 8b are the increased tilt numbers to the northeast and south of KIWA. Recall the hybrid scan of VCP 12 is not restricted to the 4 lowest tilts and has a finer elevation angle resolution at low levels than operational hybrid scans.

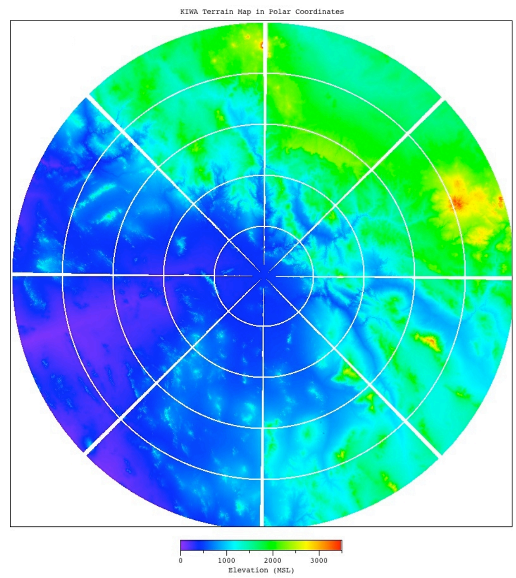

Fig. 6 A polar DEM grid as remapped from a Cartesian grid for KIWA. Range rings are every 50 km and azimuths every 45°.

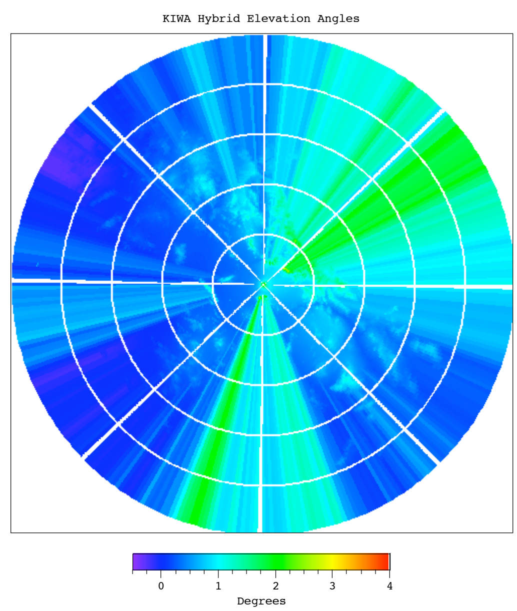

Fig. 7 The hybrid elevation angles for KIWA. Range rings are every 50 km and azimuths every 45°.

2. SUMMARY

The automated beam occultation algorithm, HybScan, and sample output are presented in this paper. The algorithm is designed as a highly adaptable and accurate scheme for computing hybrid elevation angle data sets independent of radar type and scan strategy. User defined parameters such as grid resolution and size allow for flexibility. The user may also control the definition of the hybrid elevation angle by setting the beam bottom clearance and occultation requirements. Hybrid elevations angle data sets for the WSR-88D network were computed from a high-resolution terrain data set leading to greater accuracy in determining hybrid elevation angles and hybrid scans. Sample output from this data set is given and includes polar DEM grids, hybrid elevation angle plots, computed hybrid scans for VCP 12, and operation hybrid scans.

3. ACKNOWLEGEMENTS

Major funding for this research was provided under the Aviation Weather Research Program NAPDT (NEXRAD Algorithms Product Development Team) MOU and partial funding was provided under NOAA-OU Cooperative Agreement #NA17RJ1227 and through the collaboration with the Central Weather Bureau of Taiwan, Republic of China.

4. REFERENCE

Doviak, R.J., and D.S. Zrnic, 1993: Doppler Radar and Weather Observations, 2nd Edition, Academic Press, 562 pp.

O'Bannon, 1997: Using a 'terrain-based' hybrid scan to improve WSR-88D precipitation estimates. *Preprints, The 28th International Conference on Radar Meteorology*, September 7-12, 1997, 506-507

Fulton, R. A., J. P. Breidenbach, D.-J. Seo, D. A. Miller, and T. O'Bannon, 1998: The WSR-88D rainfall algorithm. Wea. Forecasting, 13, 388-395

Kucera, P. A., W. F. Krajewski, C. B. Young 2004: Radar Beam Occultation Studies Using GIS and DEM Technology: An Example Study of Guam. *J. Atmos. Oceanic Technol.*: Vol. 21, No. 7, pp. 995–1006.

Pellarin, T., G. Delrieu, G.-M. Saulnier, H. Andrieu, B. Vignal, J.-D. Creutin, 2002: Hydrologic Visibility of Weather Radar Systems Operating in Mountainous Regions: Case Study for the Ardèche Catchment (France). *J. Hydrom.*: Vol. 3, No. 5, pp. 539–555.

Westrick, K. J., C. F. Mass, B. A. Colle, 1999: The Limitations of the WSR-88D Radar Network for Quantitative Precipitation Measurement over the Coastal Western United States. *Bull. Amer. Meteor. Soc.*: Vol. 80, No. 11, pp. 2289–2298.

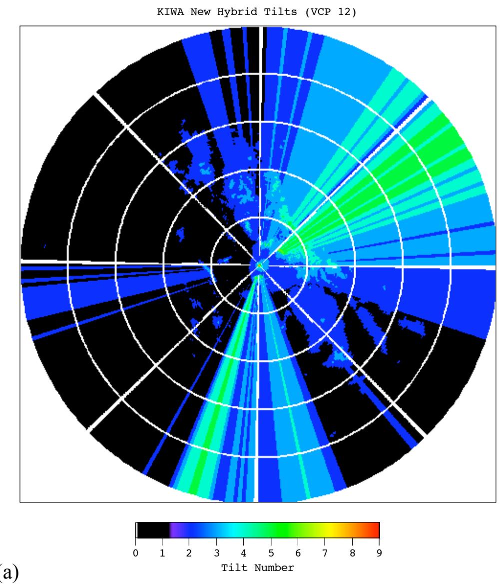

(a)

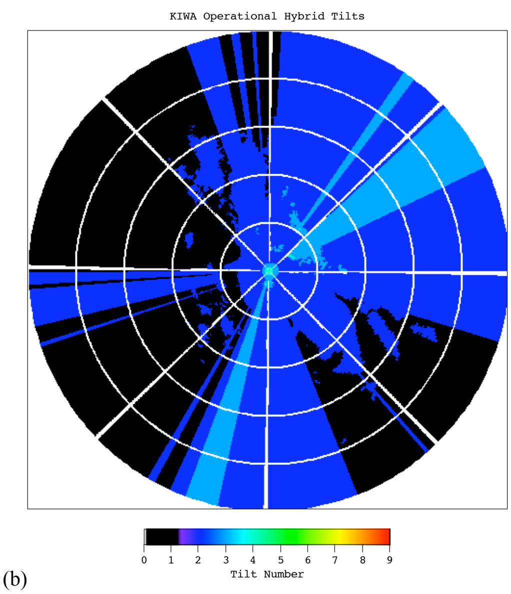

(b)

Fig. 8 Hybrid scans for KFTG generated for VCP 12 (a) and for operational WSR-88D hybrid scans (b). Range rings are every 50 km and azimuths every 45°.

Tilt #	1	2	3	4	5	6	7	8	9	10	11	12	13	14
VCP 11	0.5	1.45	2.4	3.35	4.3	5.2	6.2	7.5	8.7	10.0	12.0	14.0	16.7	19.5
VCP 21	0.5	1.45	2.4	3.35	4.3	6.0	9.9	14.6	19.5					
VCP 31	0.5	1.5	2.5	3.5	4.5									
VCP 32	0.5	1.5	2.5	3.5	4.5									
VCP 12	**0.5**	**0.9**	**1.3**	**1.8**	**2.4**	**3.1**	**4.0**	**5.1**	**6.4**	**8.0**	**10.0**	**12.5**	**15.6**	**19.5**
VCP121	**0.5**	**1.45**	**2.4**	**3.35**	**4.3**	**6.0**	**9.9**	**14.6**	**19.5**					

Table 1 Elevation angles (°) in operational VCPs for WSR-88Ds.